PVC/MBS Blends with Small Concentrations of PET: Failure Processes in Thin Films During Uniaxial Tension

J. X. LI,[1] M. V. TWIGG,[2,*] A. HILTNER,[1,†] and E. BAER[1]

[1]Department of Macromolecular Science and Center for Applied Polymer Research, Case Western Reserve University, Cleveland, Ohio 44106; [2]EVC International, Boulevard du Souverain 360, B-1160 Brussels, Belgium

SYNOPSIS

The effects of small concentrations of poly(ethylene terephthalate) (PET) particles on the failure of poly(vinyl chloride) blended with a (methacrylate–butadiene–styrene) impact modifier (PVC/MBS) were studied. The failure processes arising from isolated and interacting particles were observed *in situ* in the optical microscope during tensile deformation. At low PET content (< 0.5%), voids grew around individual particles without particle–particle interaction. Subsequently, a stable neck developed, and the material experienced relatively large deformation before fracture. With increasing PET content and increasing particle size, particle–particle interactions were observed. At higher PET content (≥ 1%), the neck was not stable and fracture occurred during neck formation. Materials with larger particles exhibited neck instability and fracture at lower PET content. © 1994 John Wiley & Sons, Inc.

INTRODUCTION

Poly(vinyl chloride) (PVC) is the second largest thermoplastic by volume in the United States.[1] The major applications of PVC are in construction and packaging. Construction products are designed for long lifetimes, while the packaging materials usually can be recycled into such items as PVC bottles.[1] In the waste stream, PVC is often combined with other thermoplastics such as poly(ethylene terephthalate) (PET), polyethylene (PE), and polypropylene (PP). Although PVC and PET are easily separated from PE or PP by water flotation due to large differences in the densities, PVC cannot be separated from PET by normal flotation because of the similarity of their densities. Therefore, PVC and PET present a cross-contamination problem. Several processes have been developed to separate the PET from PVC; however, a small amount of PET contamination, about 5%, usually persists.[2-4] Since PET does not melt at PVC processing temperatures, it exists in PVC as rigid particles that can severely compromise the mechanical properties of the reprocessed PVC.

Various model systems consisting of polymer filled with rigid particles have been studied including glass bead-filled polystyrene,[5,6] polycarbonate,[7-9] and various elastomers.[10,11] Dekkers and Heikens presented *in situ* experimental observations of craze and shearband formation around isolated particles.[5-9] When good interfacial adhesion exists, the craze forms near the pole of the bead and expands into the matrix perpendicular to the loading direction.[5,6] Also, shearbands develop near the surface of the bead at a polar angle of about 45°.[7] In the case of poor interfacial adhesion, craze formation is preceded by dewetting along the interface between the bead and the matrix around the poles of the bead. Craze formation occurs at the interface between the pole and equator at a polar angle about 60° and the craze grows into the matrix perpendicular to the loading direction.[5,6] The angle of craze formation depends on the degree of interfacial adhesion, the properties of polymer matrix and rigid filler, and the diameter of the inclusion.[9] Shearband formation in a poorly adhering system is also preceded by dew-

* Present address: Johnson Matthey PCL, Two Orchard Road, Royston, Hertfordshire, SG85HE England.
† To whom correspondence should be addressed.

Journal of Applied Polymer Science, Vol. 52, 285–299 (1994)
 CCC 0021-8995/94/020285-15

etting along the interface between the bead and the matrix.[7]

For many glassy polymers, postyield fracture is initiated from diamond-shaped voids that grow from defects in the drawn material under uniaxial tension.[12,13] Walker and Haward[14,15] studied the formation and growth of an isolated diamond-shaped void in PVC as the fracture mechanism for this material. Such a diamond-shaped void can grow from a spherical inclusion by tearing both perpendicular and parallel to the loading direction.

Information about *in situ* failure processes in particulate-filled systems is very limited. Gent and co-workers[11,16] studied the interaction between two glass particles in an elastomer. Huang and Kinloch[17] analyzed a model system of rubber-modified epoxy polymer, also emphasizing interaction between two particles. Zhuk et al.[18] examined multivoid coalescence in an epoxy resin with glass beads, and in an entirely different system, Mikhler et al.[19] studied the microdeformation of HDPE filled with aluminum hydroxide particles.

This study was concerned with the loss of mechanical properties in PVC/MBS blends contaminated with small concentrations of PET particles, a major problem in the recycle of PVC bottles. Although the amount of PET contamination can be reduced to about 5% relatively easily, further reduction becomes prohibitively expensive, and it is of interest to know the limits on the amount of contamination that can be tolerated. To understand the effects of low PET concentrations, the failure mechanisms are described for isolated and interacting particles from *in situ* microscopic observations. In particular, the effects of PET particle size and concentration are examined.

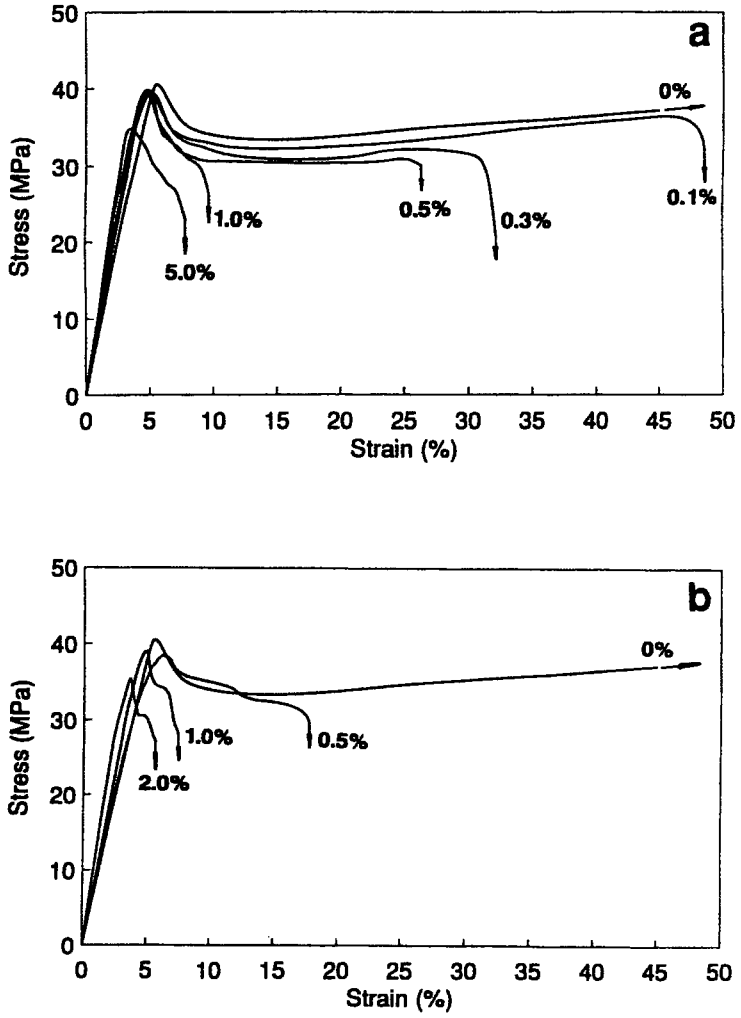

Figure 1 Stress–strain curves of PVC/MBS with PET particles: (a) PVC/MBS with small PET particles; (b) PVC/MBS with large PET particles.

Table I Size and Concentration Effects of PET Particles

Particle Size	PET (%)	Initial Length of Neck Region (mm)	Neck Type	Neck Development at the Fracture	Particle Effect
	0.0	10.0	Diffuse neck[a]	Strain hardening	None
Small (0.1 mm)	0.1	3.2	"	Neck propagation	Isolated
	0.3	2.6	"	"	"
	0.5	2.1	"	"	"
	1.0	1.2	"	Neck formation	Interaction
	2.0	1.5	"	"	"
	5.0	0.6	Local neck[b]	"	"
Large (0.3 mm)	0.5	0.8	"	"	"
	1.0	0.6	"	"	"
	2.0	0.5	"	"	"
	5.0	0.4	"	"	"

[a] Diffuse Neck
[b] Local neck

EXPERIMENTAL

Bottle-grade poly(ethylene terephthalate) (PET) (Goodyear CLEARTUF 7270) was ground and separated into two particle sizes by passing it through 80 and 120 mesh sieves. The particle-size distribution was 0.05–0.2 mm for small and 0.2–0.6 mm for large particles. The particles were nearly spherical in shape with average particle sizes of 0.1 mm (small) and 0.3 mm (large). The mixture of 100 parts of poly(vinyl chloride) (PVC) (BF Goodrich Geon 110 × 334), 15 parts of a methacrylate–butadiene–styrene (MBS) impact modifier (Paraloid BTA 733), 3 parts TM-181 tin stabilizer, 5 parts Paraloid K120N acrylic processing aid, and 0.5 parts stearic acid lubricant was dry-blended with 0, 0.1, 0.2, 0.3, 0.5, 1.0, 2.0, and 5.0 wt % of PET particles. The dry blend was roll milled at 190°C for 5 min and subsequently compression-molded at 230 psi at the same temperature.

Samples, 30 × 1.5 × 0.8 mm, were cut from the compression-molded sheets and polished to obtain a 10 mm gauge in the center region. The tensile properties were determined using a Minimat tensile tester at a crosshead speed of 0.02 mm/min. Optical micrographs were taken during extension. Fractured specimens were coated with 90 Å gold and examined in a JEOL JSM-840A scanning electron microscope (SEM).

A scanning acoustic microscope (SAM) (Olympus UH3) was used to study particle–particle interactions in the stress-whitened regions in the de-

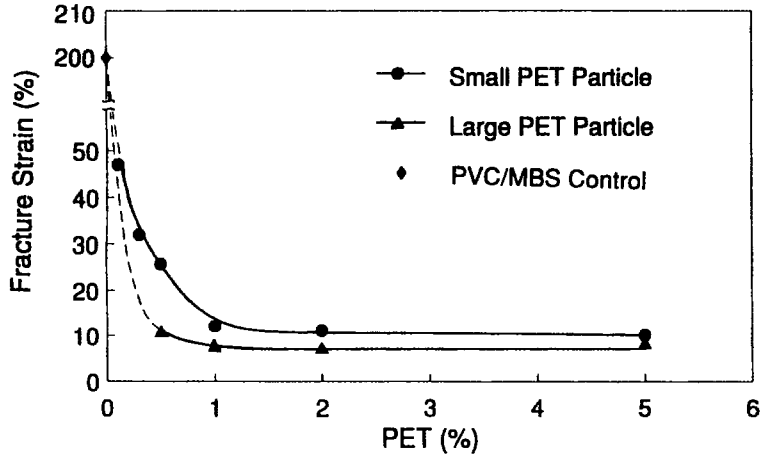

Figure 2 Effect of PET particle size and concentration on the fracture strain.

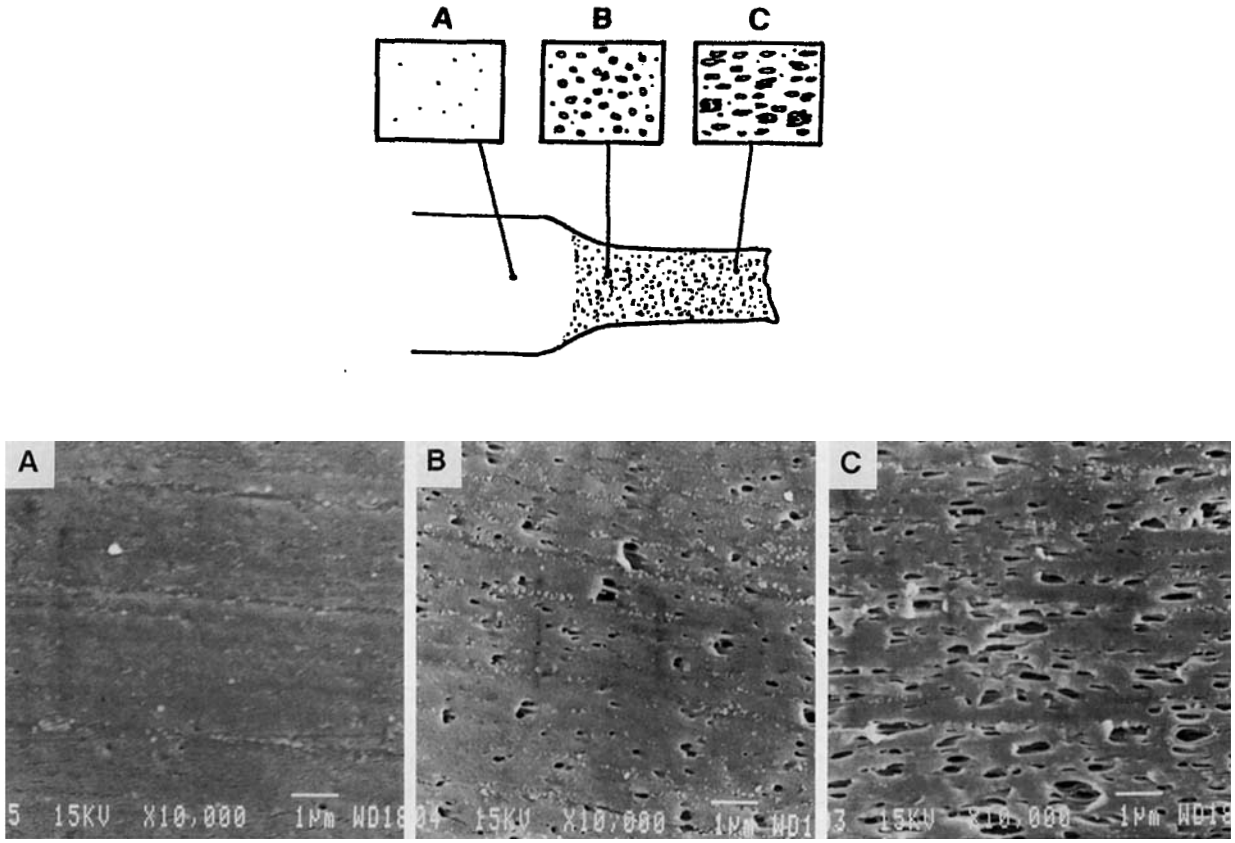

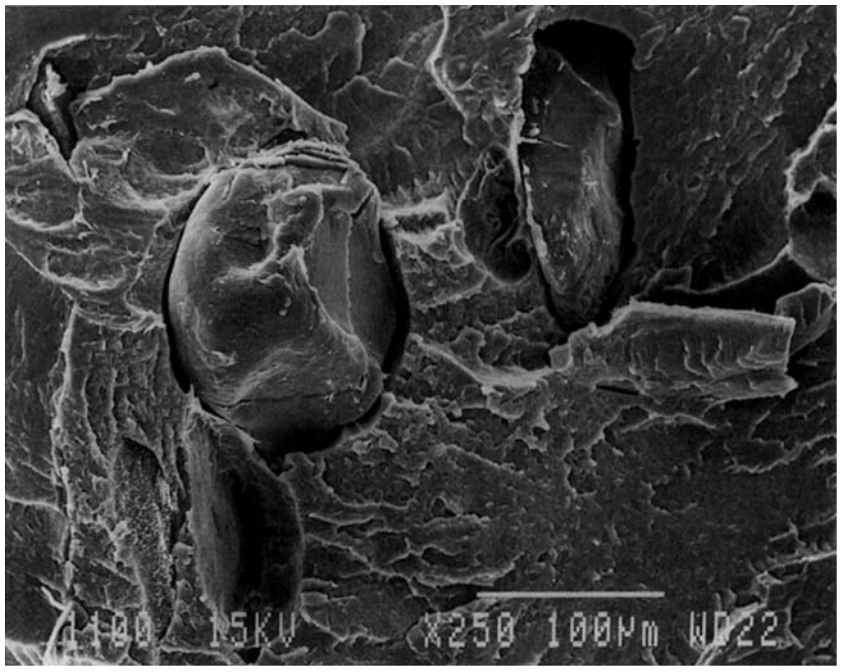

Figure 4 SEM micrograph of a cryogenic fracture surface of PVC/MBS with 1.0% small PET particles. Poor interfacial adhesion between PVC/MBS blend and PET particles was observed.

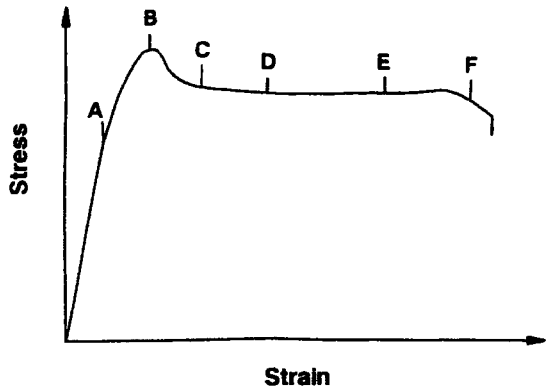

Figure 5 Schematic stress–strain curve of PVC/MBS with less than 0.5% small PET particles. The positions indicate the typical failure processes around an isolated PET particle: Initial debonding started at the poles of the particle at position A; crazing and shearbanding initiated at the interface of the particle and the matrix as debonding ceased (A → B); voids grew around the debonded particle (B → E); and final failure occurred by microscopic tearing from a diamond-shaped void (E → F).

formed specimens. The SAM can be used to examine both the internal and the subsurface structures of opaque materials. Since samples for SAM studies must have flat smooth surfaces, thin films were compression-molded between mirror-smooth polished plates at 190°C and 200 psi for 3 min. The samples were cut into a dog-bone shape with a uniform thickness of 0.35 mm. The specimen was extended 5% in a hand stretcher and examined in the SAM with 200 and 600 MHz lenses.

RESULTS AND DISCUSSION

Stress–Strain Behavior

Figure 1(a) and (b) show the effects of both PET concentration and particle size on the stress–strain behavior of the PVC/MBS blend. The Young's modulus increased with increasing PET content; the yield stress and strain did not change significantly at low PET content, but decreased at higher PET content. The fracture strain was significantly reduced from 200% in the PVC/MBS blend to 48% with the addition of only 0.1% of the small PET particles. The control specimen of the PVC/MBS blend developed a stable diffuse neck that gradually propagated through the entire 10 mm gauge length and then strain-hardened before fracture. For PVC/

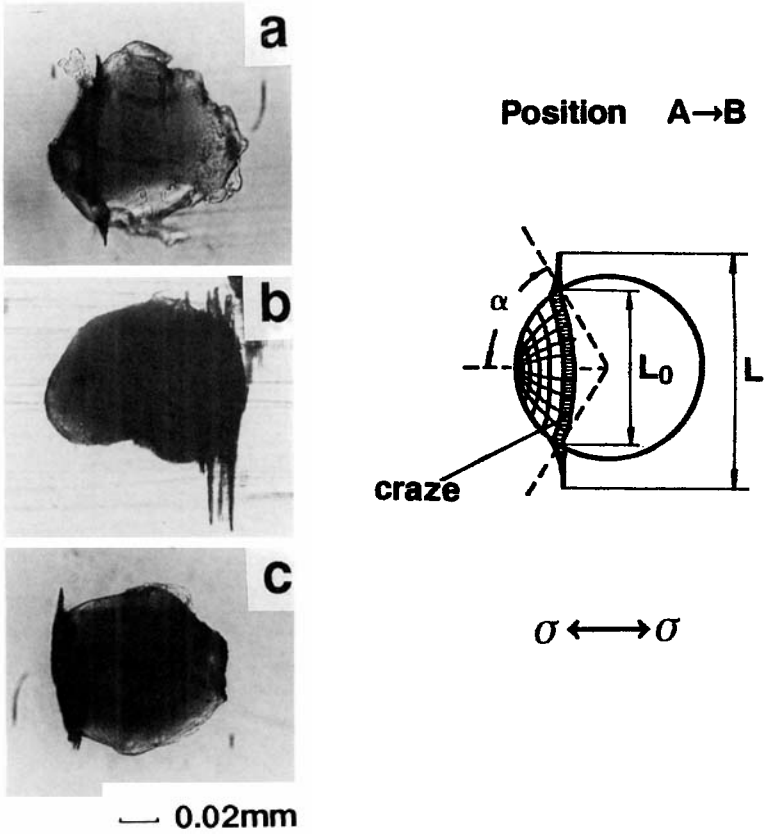

Figure 6 Debonding and craze formation around an isolated PET particle.

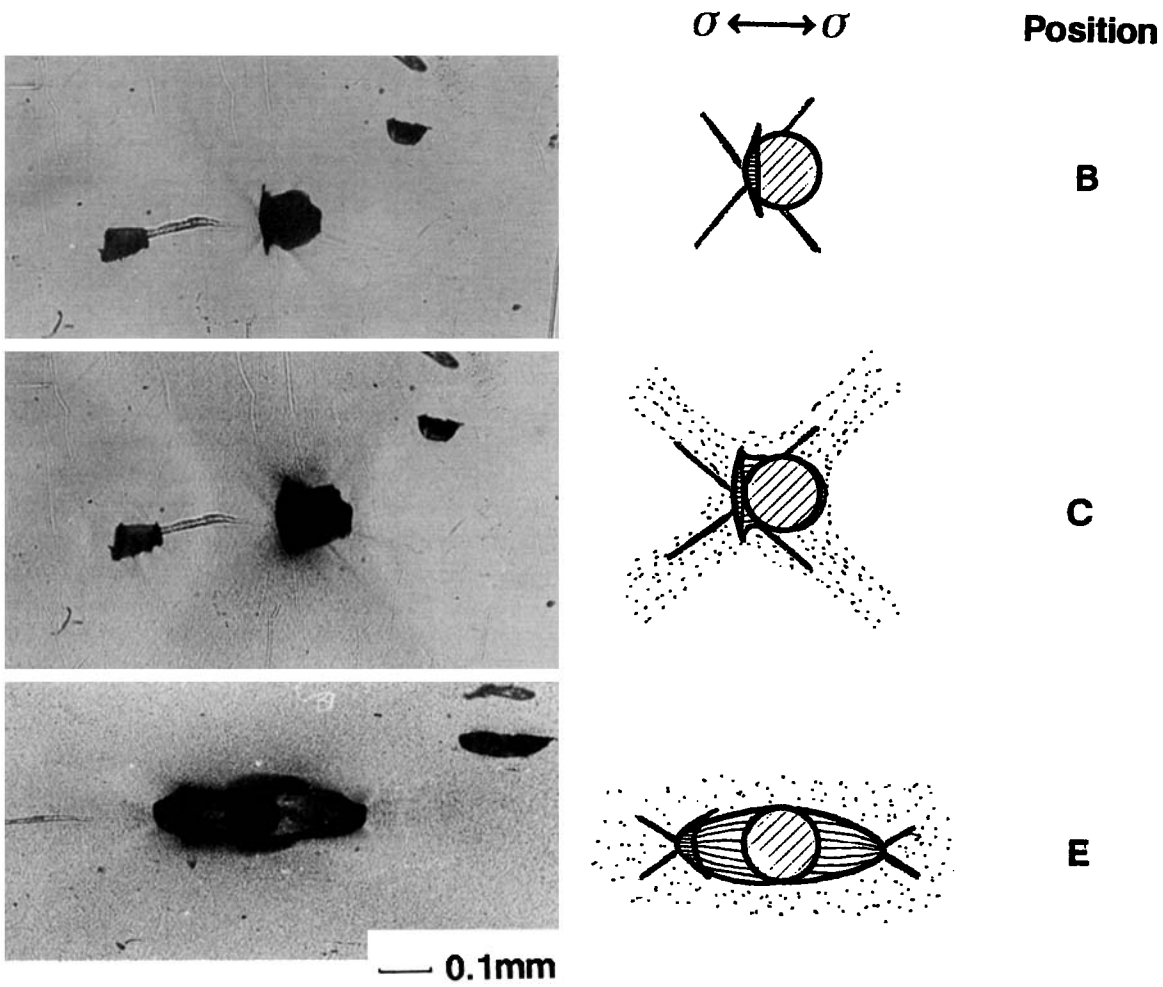

Figure 7 Shearband formation around an isolated PET particle.

MBS with PET particles, the neck became increasingly localized with increasing PET concentration and never propagated through the entire gauge length of the specimen (Table I).

The stress–strain behavior of PVC/MBS filled with the small PET particles (0.1 mm) is shown in Figure 1(a). At low PET content (0.1–0.5%), a stable diffuse neck developed, and the material fractured during neck propagation at a relatively large deformation at 28–48% strain. With increasing PET content (≥ 1.0%), the test specimens did not form stable necks and fracture occurred at strains less than 10%. With the highest concentration of PET particles (5.0%), the yielding process changed from diffuse to localized necking (Table I).

The stress–strain behavior of PVC/MBS with large PET particles (0.3 mm) is shown in Figure 1(b). The large particles caused the fracture strain to decrease more than the same concentration of small particles. The smallest concentration of large PET particles, 0.5%, was sufficient to cause necking instability. During localized necking, a macroshearband formed and fracture emanated from this band.

Figure 2 shows the effect of PET concentration on the fracture strain. For PVC/MBS with small PET particles, a gradual decrease of fracture strain was observed with increasing of PET concentration from 0.1 to 1.0%. At PET contents lower than 1.0%, stable diffuse necking was observed with relatively large fracture strains. As the PET content increased to ≥ 1.0%, stable neck propagation was no longer achieved. For PVC/MBS with large PET particles, neck instability was observed at the lowest PET content (0.5%).

Stress-whitening due to cavitation of the MBS rubber particles was observed in the neck region for both the PVC/MBS control and the PET-filled systems. The SEM micrographs of a PVC/MBS specimen deformed under uniaxial tension showed profuse cavitation in the stress-whitened region (Fig. 3). The cavities were elongated in the loading di-

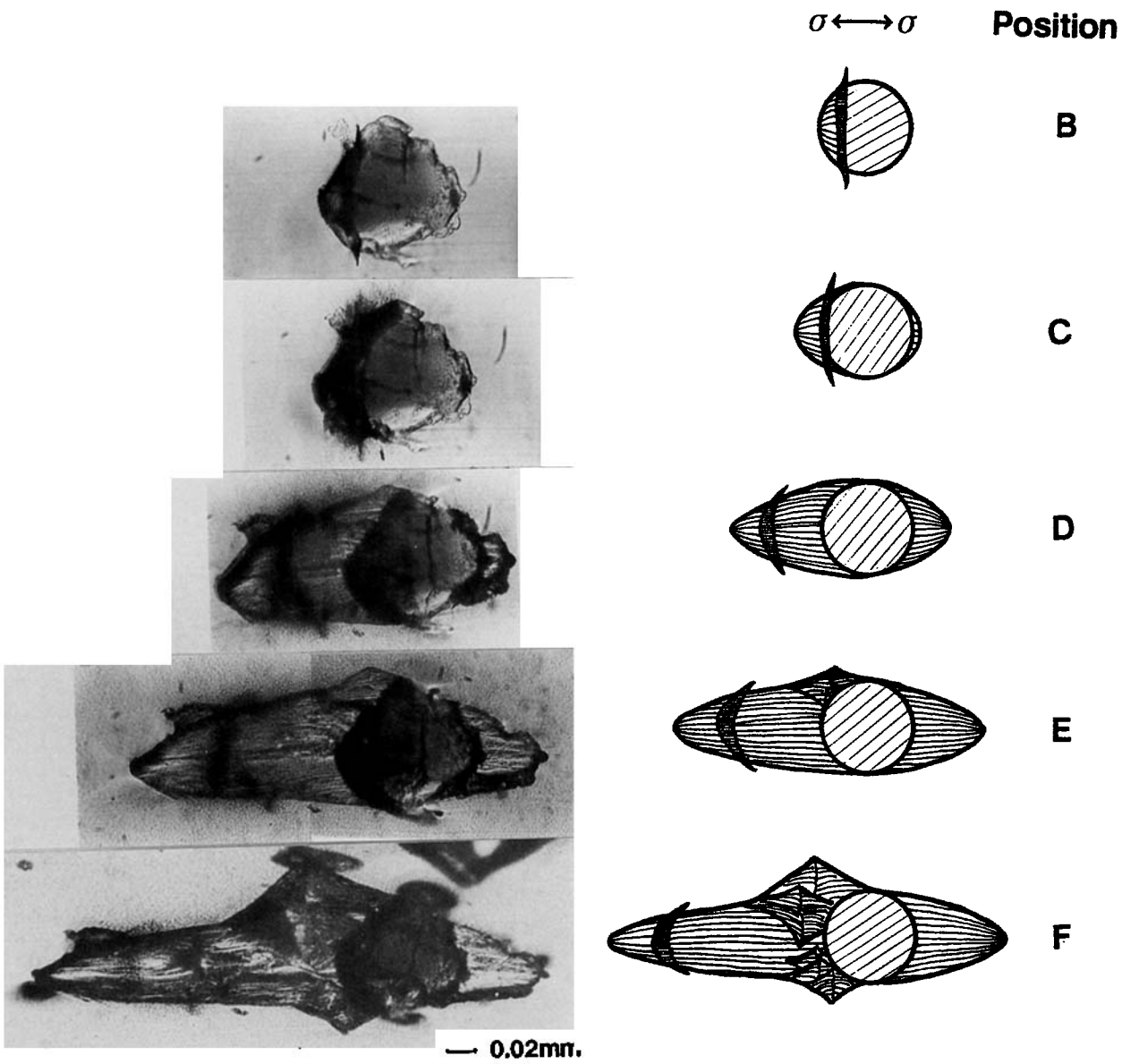

rection in the highly deformed center region and were about 0.2–1.0 μm in length. These cavities were at least 300 times smaller than the PET particles (100–300 μm), indicating that PET particles were the defect inclusions responsible for the low fracture strain of filled PVC/MBS. Furthermore, debonded regions were readily observed around the PET particles on a cryogenic fracture surface (Fig. 4), which indicated that the interfacial adhesion between the PVC/MBS matrix and the PET particles was poor.

Failure from Small Isolated PET Particles

The failure around isolated PET particles was observed only when the PVC/MBS blend contained less than 0.5% small PET particles. Figure 5 indicates on a typical stress–strain curve the initiation of failure processes around an isolated PET particle. Debonding started at the poles of the particle at position A on the stress–strain curve. Debonding did not continue around the particle; instead, crazing and shearbanding initiated at the interface between the particle and the matrix, position B. Then, voids formed in the debonded regions at the poles of the particles, position C, and continued to grow with increasing strain, positions D and E. Fracture occurred by microscopic tearing from a diamond-shaped void, position F. Detailed observations of each of these processes are discussed in the remainder of this section.

Debonding occurred at the poles of the PET particles at the end of the linear region of the stress–

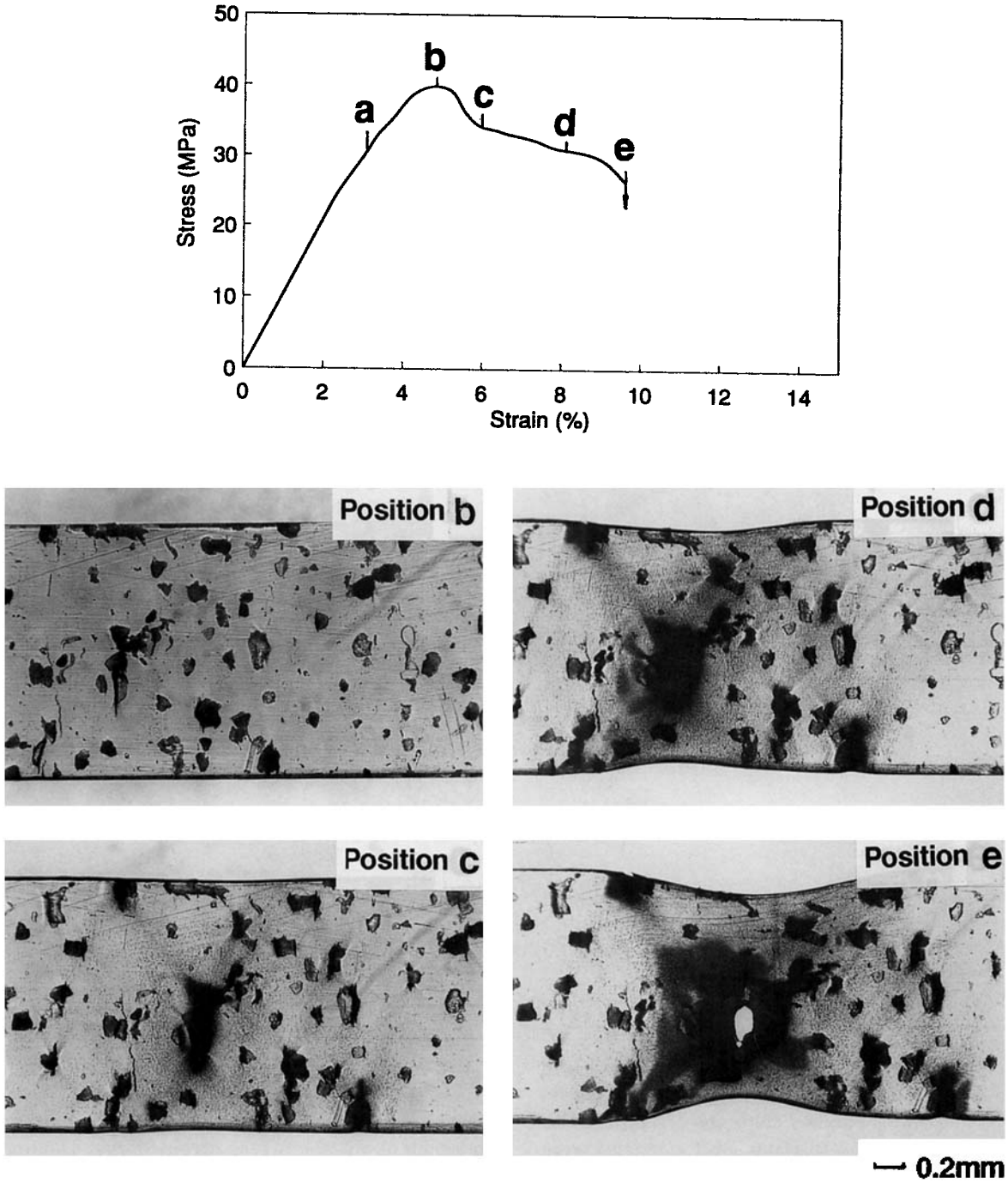

Figure 9 Optical micrographs of failure processes of PVC/MBS with 1.0% small PET particles. A diffuse neck developed and particle–particle interaction was observed in the stress-whitened region.

strain curve and continued along the matrix/particle interface toward the equator until the polar angle (α) reached 60–70°. This debonding process was very similar to that previously observed with glass bead-filled polystyrene with poor adhesion.[5,6] Circular crazes initiated at the debonding interface and lengthened perpendicular to the loading direction [Fig. 6(a) and (b)]. Propagation of the crazes stopped when shearbands appeared around the particles. The maximum ratio of the total length of the

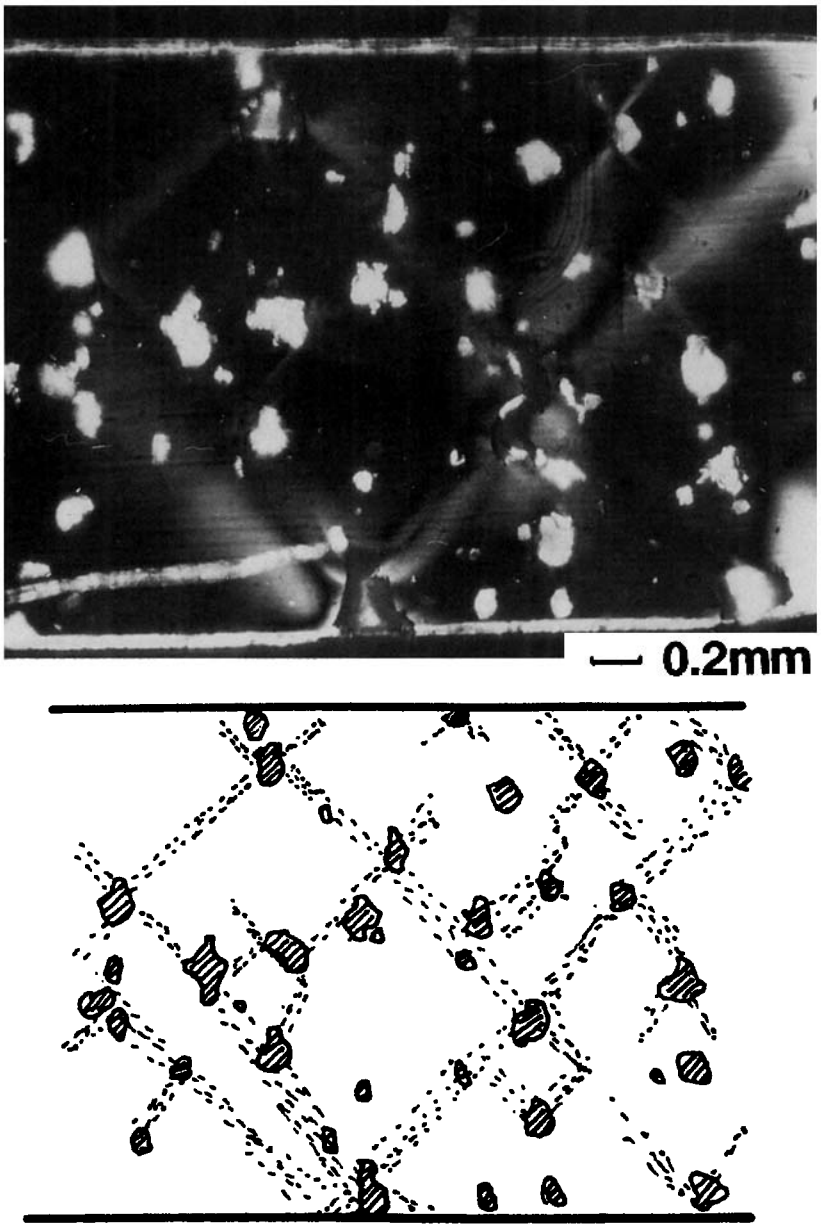

Figure 10 Optical micrograph of shearband coalescence in PVC/MBS with 1.0% small PET particles under crossed polars.

craze to the diameter of the particle where the craze initiated (L/L_0) was about 1.6. Multiple crazes were also observed along the debonded interface [Fig. 6(b)]. This was not seen in the previous studies with glass beads[5,6] and might have been caused by multiple stress concentration sites in the rough surface of the PET particles, as observed in both optical microscopy and SEM. Occasionally, crazes were also noted at the poles of the particles [Fig. 6(c)].

At the maximum in the stress–strain curve, position B, shearbands appeared at the debonded interfaces when the matrix material reached the yield point (Fig. 7). A similar observation was made in glass bead-filled polycarbonate with poor interfacial adhesion.[7] At a very low PET content, the shearbands grew from debonded PET particles with little or no interaction with shearbands from adjacent particles, position C. The initial angle of the shearbands ranged between 50 and 60°. The angle decreased to 20–35° as the neck propagated due to the large extension of the matrix polymer, position E. The shearbands became increasingly difficult to ob-

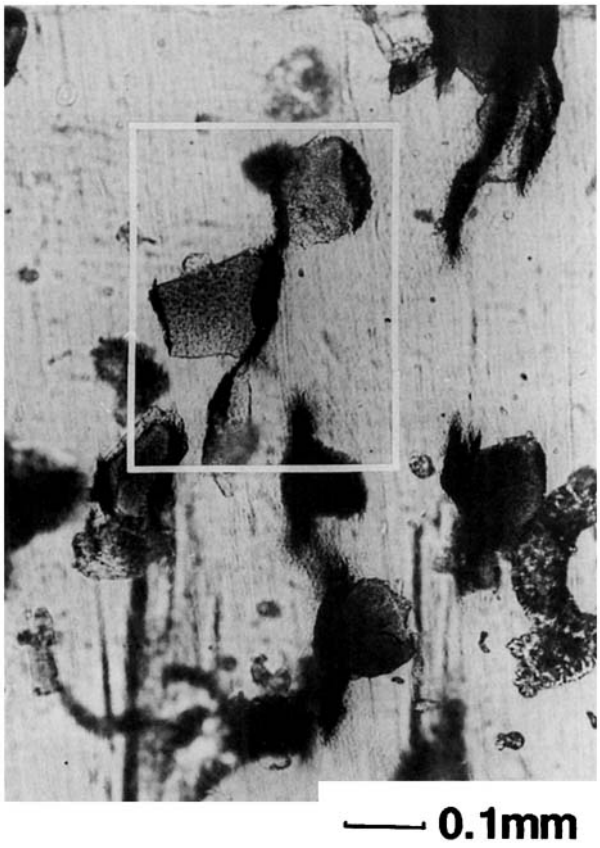

Figure 11 Optical micrograph of craze coalescence in PVC/MBS with 5.0% small PET particles.

serve as the strain increased because of the overall development of stress-whitening.

Voids formed around the debonded particles during neck formation (Fig. 8). During neck propagation, these voids expanded into an ellipsoidal shape along the loading direction. The maximum length of these ellipsoidal voids was about three times the original particle diameter. During void growth, the preexisting crazes were distorted due to the plastic deformation in the matrix,[5,8] position D. Diamond-shaped voids were created after the ellipsoidal voids had reached a critical size at a local strain of about 200%, position E. Since this strain was equal to the fracture strain of the matrix polymer, local tearing failure occurred and several crack fronts propagated from the diamond-shaped void. In the previously described diamond-shaped void, only a single crack front developed.[14,15] The appearance of multiple crack fronts was an indication of a more complicated microtearing failure process. As the crack front from the diamond-shaped void penetrated through the thickness of the specimen, the tensile stress dropped. The local strain around the particle was about 280% at position F in Figure 8.

Failure from Interacting Small PET Particles

Failure processes involving interacting particles were observed in PVC/MBS with ≥ 1.0% small PET particles. The first irreversible deformation process was again formation of crazes near the poles of the particles at position a in Figure 9. For the PVC/MBS blend with 1.0% small PET particles, shearbands initiated around the particles at the maximum in the stress–strain curve, position b. However, the shearbands began to interact slightly after the yield point had been reached. The interacting shearbands were most easily seen under crossed polars (Fig. 10). As the shearbands further coalesced, they formed the dark areas seen in unpolarized light at position c in Figure 9. As the strain increased further, ligaments of drawn matrix between debonded particles fractured, and tearing failure initiated from the large resulting voids, positions d and e. The local strain around the particle when fracture initiated was about 200%.

Crazes were also the first deformation observed in PVC/MBS with 5% small PET particles. However, the particles were close enough in this composition for crazes from nearby particles to interact and join together (Fig. 11). Subsequently, a macro-shearband formed at just past the maximum in the stress–strain curve, position b in Figure 12, as a result of localized shearband coalescence. This was accompanied by stress-whitening and complete loss of transparency in this region, position c. An unstable localized neck then developed along the macro-shearband at position d. Tearing fracture through the macro-shearband at position e followed when the local strain around the particles reached about 150%. Increasing particle–particle interactions when the PET content was increased from 1.0 to 5.0% were responsible for a less stable neck and a lower local strain around the particles at fracture.

One of the complications in studying the failure processes of interacting particles was the opaqueness of the specimens caused by stress-whitening. Scanning acoustic microscopy (SAM) was used to observe particle–particle interactions in the stress-whitened region and to determine the thickness reduction that resulted from nonuniform, localized deformation at the particles. The interacting strain fields in the stress-whitened area of PVC/MBS blend with 5.0% small PET particles were clearly

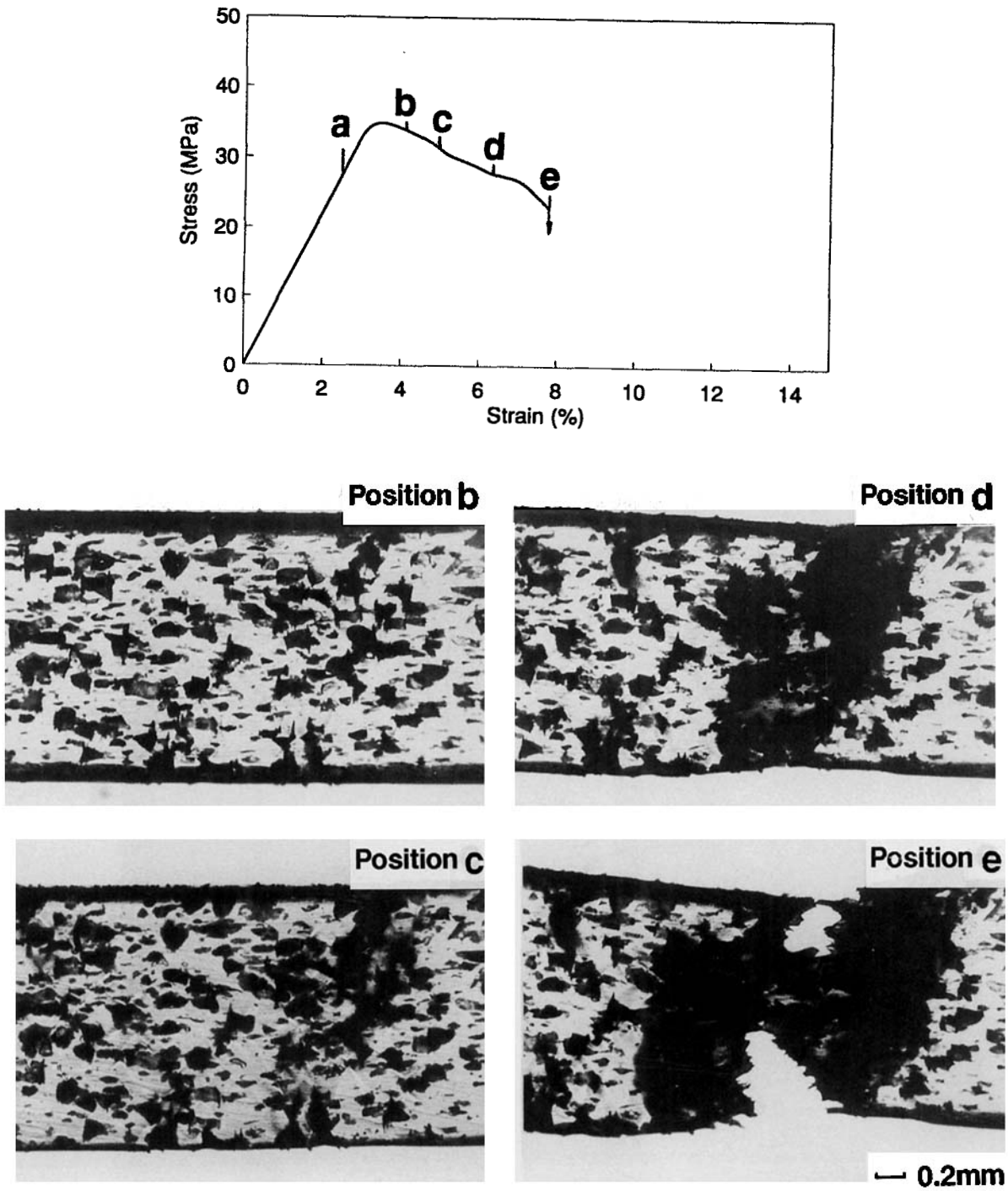

Figure 12 Optical micrographs of failure processes of PVC/MBS with 5.0% small PET particles. A localized neck formed due to particle–particle interactions.

observed in the X-Y images with a 200 MHz lens (Fig. 13). The contours concentrated around the particles represented variations in surface topology. It was possible to measure the magnitude of the thinning from X–Z images obtained with a 600 MHz lens. Acoustic scans made in the X-direction at three positions, 1, 2, and 3, produced the X–Z images included in Figure 13. The initial thickness of the

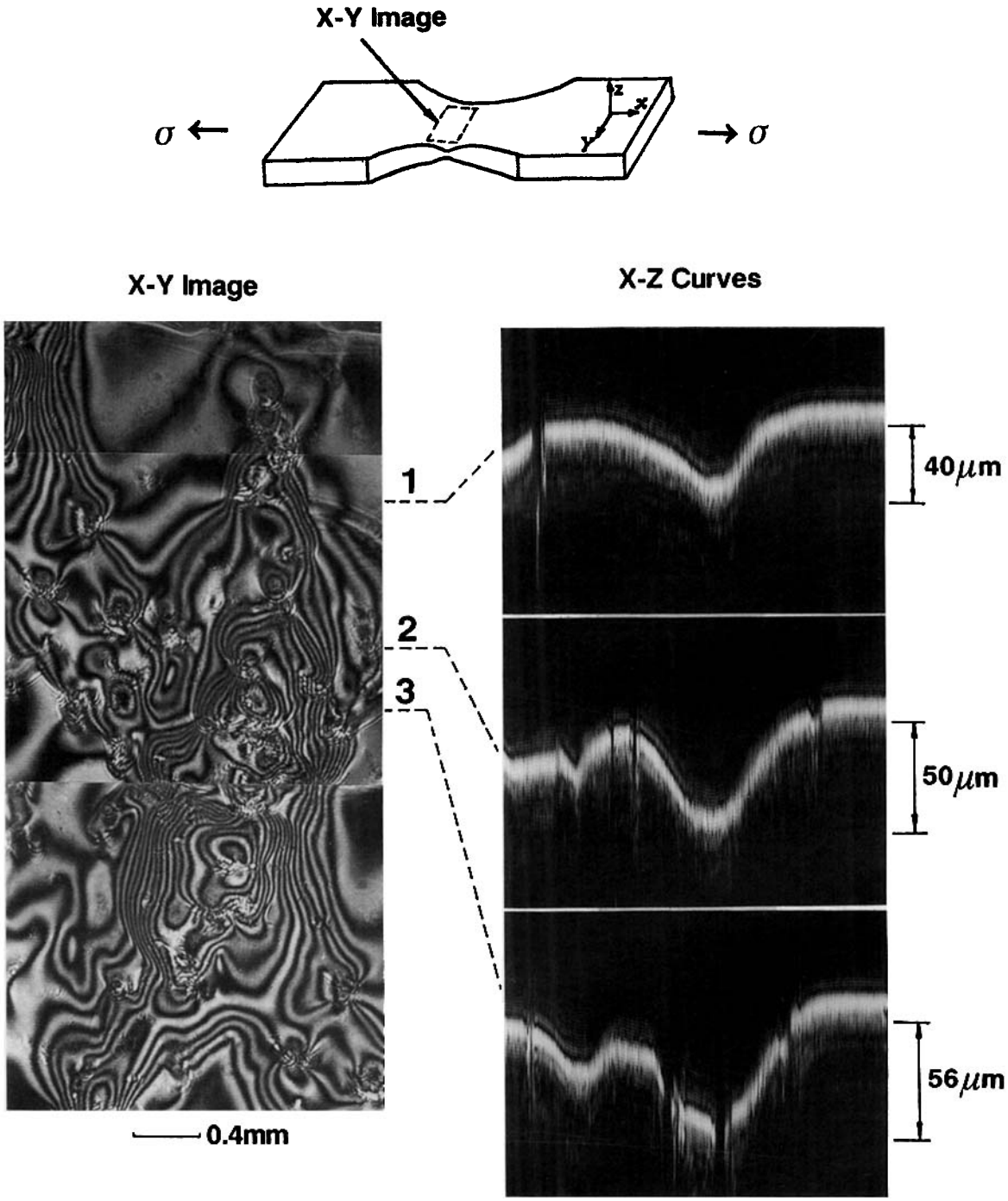

Figure 13 SAM observation of PVC/MBS with 5.0% small PET particles. The particle–particle interaction in the stress-whitening area was clearly observed in the *X–Y* image obtained with a 200 MHz lens. The thickness reduction in this highly plastically deformed region was shown in the *X–Z* curves obtained with a 600 MHz lens.

specimen was about 0.35 mm. The maximum thickness reduction in the stress-whitened region was about 30% of the original thickness of the specimen at a tensile strain of only about 5%. This observation confirmed that particle–particle interactions generated high localized plastic deformation leading to early fracture.

In summary, two types of failure mechanisms were observed for PVC/MBS with small PET particles (0.1 mm). At low PET content (0.1–0.5%),

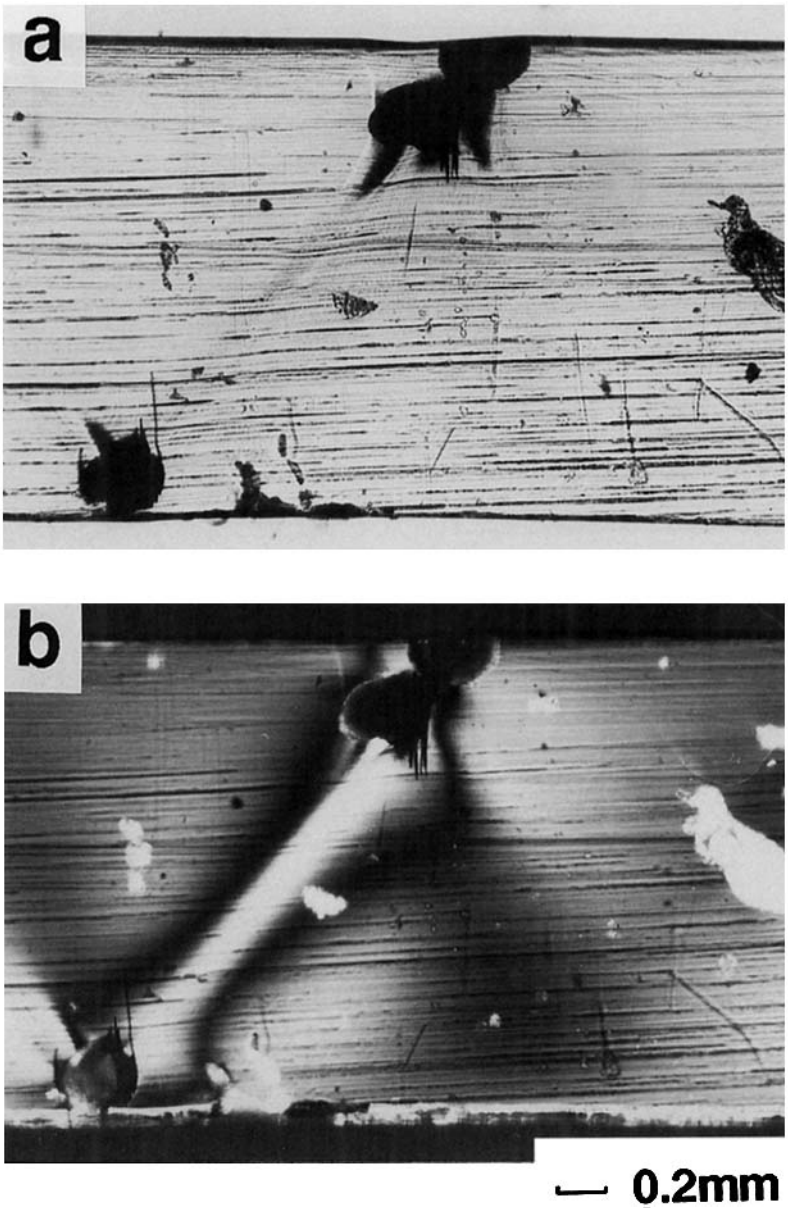

Figure 14 Optical micrographs of particle–particle interaction in PVC/MBS with 0.5% large PET particles: (a) transmitted light; (b) with crossed polars.

failure occurred at isolated particles. The voids grew individually and fracture initiated from isolated PET particles after stable neck propagation. At high PET content ($\geq$ 1%), particle–particle interactions induced coalescence of crazes, shear bands, and, finally, voids. Premature fracture by tearing prevented stable neck propagation.

Failure from Large PET Particles

Failure involving interacting particles was observed in all the PVC/MBS blends with large PET particles (0.3 mm). The deformation mechanism was similar to that with 5.0% small particles. Multiple crazes were observed more frequently around large particles. When the shearbands formed, the particles were large enough that a single macro-shearband grew across the entire width of the specimen. Figure 14 shows this kind of macro-shearband in PVC/MBS with 0.5% large PET particles. Localized necking typically propagated from such a macro-shearband induced by two particles.

Similar interactions were also observed in the PVC/MBS with 1.0% large PET particles (Fig. 15).

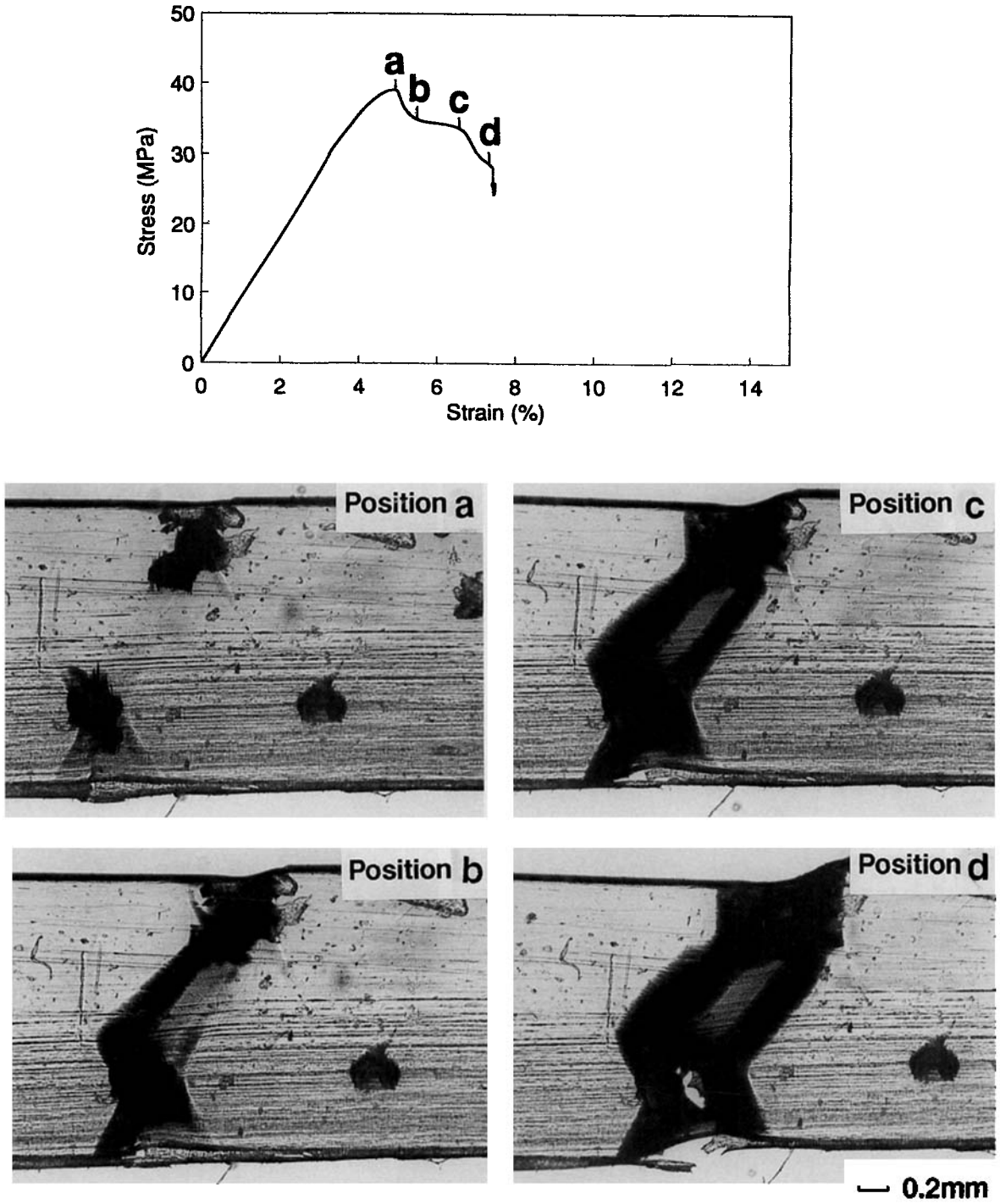

Figure 15 Optical micrographs of failure processes of PVC/MBS with 1.0% large PET particles. A local neck formed due to particle–particle interactions.

The shearbands that formed at position a on the stress–strain curve interacted to create a macro-shearband across the entire width of the specimen at position b from which the localized neck formed at position c. Subsequently, tearing fracture occurred at position d as the local strain around the

particles reached about 90%. This was a much lower strain than with small PET particles (200%) at the same PET concentration.

CONCLUSIONS

1. The stress–strain behavior of PET particle-filled systems are described using two concentration categories: At low PET content ($< 1\%$), a stable neck develops and the materials have relatively larger fracture strains, whereas at high PET content ($\geq 1\%$), the materials do not develop a stable neck, which results in premature fracture during neck formation.
2. Failure processes around an isolated PET particle are described in PVC/MBS with $\leq 0.5\%$ of the small PET particles. With increasing deformation, initial debonding starts at the poles, then crazing and shearbanding initiate when debonding ceases, followed by void growth in the debonded region and, finally, failure by tearing.
3. Particle–particle interactions are observed during the failure processes in PVC/MBS with $\geq 1.0\%$ of the small PET particles and $\geq 0.5\%$ of the large PET particles. Particle–particle interactions, which increase with increasing PET content, induce localized craze, shearband, and void coalescence. These effects inhibit the propagation of a stable neck throughout the specimen and cause premature fracture by tearing.
4. The amount of PET contamination that can be tolerated in PVC is very small. When the PET particles are on a size scale typically obtained by conventional grinding techniques, 0.1–0.3 mm, even a concentration of 0.1% particles by weight results in a significant loss of ductility.

The authors thank Dr. Fred Lisy for assistance with the scanning acoustic microscopy. This research was supported by the BFGoodrich Co. and European Vinyls Corp. though the Edison Polymer Innovation Corp. (EPIC).

REFERENCES

1. R. J. Ehrig, Ed., *Plastics Recycling: Products and Processes,* Hanser, Oxford University Press, New York, 1992, Chap. 6.
2. I. W. Summers, B. K. Mikofalvy, and S. Little, *J. Vinyl Tech.*, **12,** 154 (1990).
3. G. Carlo, U.S. Pat. 4,884,386.
4. P. A. Toensmeier, *Mod. Plast.*, **67**(6), 15 (1990).
5. M. E. J. Dekkers and D. Heikens, *J. Mater. Sci. Lett.*, **3,** 307 (1984).
6. M. E. J. Dekkers and D. Heikens, *J. Mater. Sci.*, **18,** 3281 (1983).
7. M. E. J. Dekkers and D. Heikens, *J. Mater. Sci.*, **19,** 3271 (1984).
8. M. E. J. Dekkers and D. Heikens, *J. Mater. Sci.*, **20,** 3865 (1985).
9. M. E. J. Dekkers and D. Heikens, *J. Mater. Sci.*, **20,** 3873 (1985).
10. A. N. Gent, *J. Mater. Sci.*, **15,** 2884 (1980).
11. A. N. Gent and B. Park, *J. Mater. Sci.*, **19,** 1947 (1984).
12. N. Walker, J. N. Hay, and R. N. Haward, *Polymer,* **20,** 1056 (1979).
13. P. L. Cornes, K. Smith, and R. N. Haward, *J. Polym. Sci. Polym. Phys. Ed.*, **15,** 955 (1977).
14. N. Walker, R. N. Haward, and J. N. Hay, *J. Mater. Sci.*, **14,** 1085 (1979).
15. P. L. Cornes and R. N. Haward, *Polymer,* **15,** 149 (1974).
16. A. N. Gent and Y. C. Hwang, *J. Mater. Sci.*, **25,** 4981 (1990).
17. Y. Huang and A. J. Kinloch, *J. Mater. Sci.*, **27,** 2753 (1992).
18. A. V. Zhuk, A. Ya. Gorengerg, V. A. Topolkaraev, and V. G. Oshmyan, *Mech. Compos. Mater.*, **23,** 533 (1987).
19. G. Mikhler, Yu. M. Tovmasyan, V. A. Topolkaraev, I. L. Dubnikova, and V. Shmidt, *Mech. Compos. Mater.*, **24,** 167 (1988).

Received May 5, 1993
Accepted August 21, 1993